ELSEVIER

Materials Science and Engineering A269 (1999) 136–141

MATERIALS SCIENCE & ENGINEERING A

www.elsevier.com/locate/msea

Fatigue crack initiation and fracture behavior of a copper bicrystal with a perpendicular grain boundary

Z.F. Zhang *, Z.G. Wang, Y.M. Hu

State Key Laboratory for Fatigue and Fracture of Materials, Institute of Metal Research, The Chinese Academy of Sciences, 72 Wenhua Road, Shenyang 110015, People's Republic of China

Received 20 November 1998; received in revised form 15 March 1999; accepted 22 March 1999

Abstract

By cyclically deforming a [$\bar{5}$913]⊥[$\bar{5}$79] copper bicrystal with a perpendicular grain boundary (GB), the fatigue crack initiation and fracture behavior were investigated. It was found that only the primary slip systems were activated on both G1[$\bar{5}$913] and G2[$\bar{5}$79] grains including the vicinity of the GB at axial plastic strain range of 1.8×10^{-4}–2.56×10^{-3}. By observing the surface and fractography, it was confirmed that the fatigue cracks always nucleated and propagated along the GB, and displayed an obvious tendency on different surfaces. On the front surface of the bicrystal, the intergranular cracking was more preferential than that on the lateral surface, even though the geometrical conditions among PSB, GB and stress axis on the lateral surface claimed to enhance cracking are more close to those proposed by Christ (Mater. Sci. Eng. A117 (1989) L25). Based on the experimental results above, the effect of the interaction of PSB with GB and stress axis on intergranular fatigue cracking in the bicrystal is discussed. It is suggested that Christ's geometrical conditions for intergranular cracking might be further developed and the plastic strain incompatibility near the GB should play a more important effect on intergranular fatigue cracking.

Keywords: Copper bicrystal; Cyclic deformation; Grain boundary; Fractography; Intergranular cracking

1. Introduction

Intergranular cracking is an important fatigue damage mode in polycrystals during cyclic deformation [1–3]. It has been recognized that the overall plastic strain was carried out by persistent slip bands (PSBs) which often terminated at the large-angle grain boundaries (GBs) in bicrystals [4–8] or polycrystals [1–3]. Mughrabi et al. [9] defined the interaction of PSBs with GBs as the PSB–GB mechanism for intergranular fatigue damage. However, the factors affecting the intergranular fatigue cracking are very complicated, such as grain size, GB structure, the misorientation between neighboring grains. Christ [10] considered that the interaction angles among PSB, GB and stress axis should play an important role in intergranular cracking. By stress analysis near the GB, a geometrical condition for intergranular cracking was proposed, i.e. the interaction angles (α, β) of PSB with stress axis and GB favorable to intergranular cracking are 45 and 70.5°, respectively. Recently, Hu and Wang [4] investigated intergranular fatigue cracking feature by using a [$\bar{3}$45]⊥[$\bar{1}$17] copper bicrystal with a perpendicular GB. They found that the Christ's geometrical conditions for intergranular cracking was also suitable to the [$\bar{3}$45]⊥[$\bar{1}$17] copper bicrystal. However, secondary or multiple slip spread all over the bicrystal surface and may have a great role in intergranular fatigue cracking. In this paper, a group of copper bicrystal specimens which contain typical single-slip-oriented crystals and a GB approximately perpendicular to the stress axis were designed to further clarify intergranular fatigue cracking mechanism.

2. Experimental procedure

A bicrystal with the size of $150\times50\times10\text{mm}^3$ was grown from OFHC copper of 99.999% purity by the

* Corresponding author.
E-mail address: zhfzhang@imr.ac.cn (Z.F. Zhang)

0921-5093/99/$ - see front matter
PII: S0921-5093(99)00149-5

Bridgman method in a horizontal furnace, and the GB was along the growing direction. Some fatigue specimens with a GB plane approximately perpendicular to the stress axis were spark-machined from the bicrystal plate, and the gauge size is $16 \times 6 \times 3\text{mm}^3$ as shown in Fig. 1a. By the X-ray Laue back-reflection method, the orientations of the two component crystals in the bicrystal were determined as G1$[\bar{5}913]$ and G2$[\bar{5}79]$, respectively, which are oriented for typical single slip. The crystallographic relations of the primary slip planes with GB in the bicrystal are shown in Fig. 1b. Clearly, the geometrical conditions among the primary slip plane, GB and the stress axis on the front surface are different from those on the lateral surface. Before cyclic deformation, all the bicrystal specimens were electropolished carefully for surface observation. Cyclic push–pull tests were performed on a Shimadzu servo-hydraulic testing machine under constant plastic strain control at room temperature in air. A triangular wave with a frequency range of 0.05–0.3 Hz was used. The applied axial plastic strain amplitudes ($\Delta\varepsilon_{pl}/2$) are in the range of 1.8×10^{-4}–2.56×10^{-3}. The cyclic stress–strain response and saturation dislocation observation of those bicrystals can be found in the literature [8]. After cyclic saturation or fracture, the surfaces and fractographies of the bicrystals were observed to examine the slip morphology and fatigue cracking process.

3. Results and discussion

3.1. Cyclic hardening and saturation behavior

During cyclic deformation, all the bicrystals exhibited rapid initial hardening and the followed saturation behavior in the applied strain range of 1.8×10^{-4}–2.56×10^{-3}. The axial saturation stress ranged from 62.1–63.7 to 68.5–70.8 MPa, respectively, at axial plastic strain range of 1.8×10^{-4}–1.35×10^{-3} and 1.7×10^{-3}–2.56×10^{-3}. Apparently, the cyclic stress–strain curve (CSSC) of the bicrystal displayed two plateau regions [8]. After cyclic saturation, observations on the front and lateral surfaces showed that only the primary slip systems on both G1 and G2 grains were activated including the vicinity of the GB, as shown in Fig. 2a, b. This surface slip feature is obviously different from those of $[\bar{3}45]\perp[\bar{1}17]$, $[\bar{0}01]\perp[\bar{1}49]$ and $[\bar{1}49]\perp[\bar{1}49]$ copper bicrystals [4–6]. It may be reasonable because the two component crystals in the $[\bar{5}913]\perp[\bar{5}79]$ copper bicrystal are oriented for typical single-slip. However, $[\bar{1}17]$ and [001] component crystals are oriented for double slip and multiple slip, respectively, and $[\bar{3}45]$ and $[\bar{1}49]$ component crystals are close to double-slip orientations. By using electron channeling contrast (ECC) technique [8], it was found that the ladder-like structure of persistent slip bands (PSBs) can form in both G1 and G2 grains after cyclic saturation. Therefore, the interaction of PSB with GB may occur and play an important role in intergranular fatigue cracking.

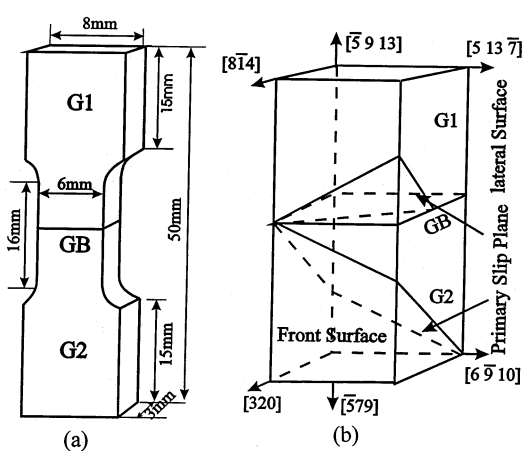

Fig. 1. Fatigue specimen and crystallographic relations of primary slip planes with GB in the $[\bar{5}913]\perp[\bar{5}79]$ copper bicrystal. (a) Fatigue specimen; (b) crystallographic relations of primary slip planes with GB.

3.2. Fatigue cracking feature of the bicrystal

After cyclic saturation, the stress began to decrease when cyclic deformation was continuously applied to the bicrystals at all the strain amplitudes. The observations on the surfaces by SEM showed that fatigue cracks had initiated and propagated along the GB plane for those bicrystals, as shown in Fig. 3a, b. In particular, it was noted that secondary slip was not activated on the bicrystal surfaces except near the intergranular fatigue crack on the lateral surface. From further observations on the two crystal surfaces, it was found that there was no fatigue crack initiating along the slip bands after GB cracking. Apparently, GB is the preferential site initiating fatigue crack in the present copper bicrystal compared with the slip bands under cyclic loading. This result is consistent with that in $[\bar{3}45]\perp[\bar{1}17]$, $[\bar{1}23]\perp[\bar{3}35]$, $[\bar{0}01]\perp[\bar{1}49]$ and $[\bar{1}49]\perp[\bar{1}49]$ copper bicrystals with a perpendicular GB [4–7].

In addition, as shown in Fig. 3a, b, the geometrical conditions among PSB, GB and stress axis can be clearly seen. During cyclic deformation, the tendency towards intergranular fatigue cracking is different at different surfaces. It is noted for all the present bicrystals that the fatigue crack always initiated along the GB on the front surface at first, and then propagated along the GB through the lateral surface, displaying a zigzag path, as shown in Fig. 3b. Those observations indicate that intergranular fatigue cracking on the front surface should be easier than that on the lateral surface in the present bicrystal.

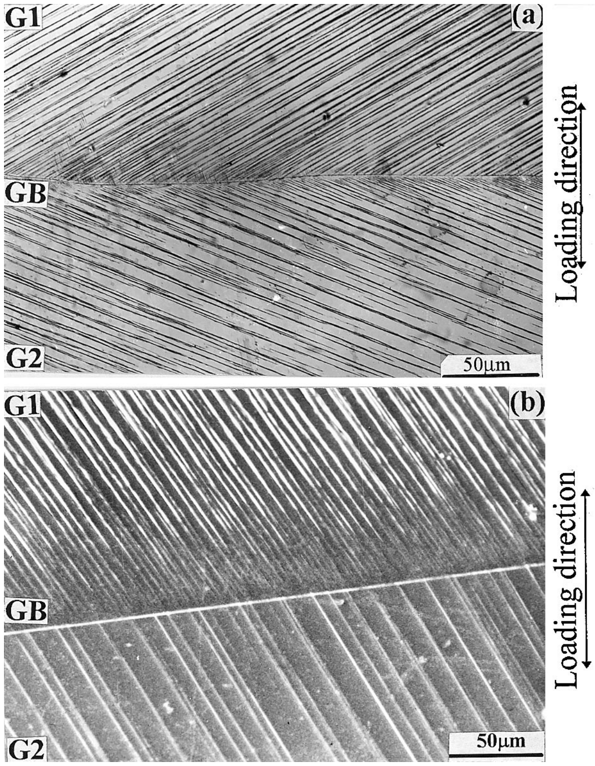

Fig. 2. Surface slip morphology of [$\bar{5}$913]⊥[$\bar{5}$79] copper bicrystal cyclically deformed at axial plastic strain amplitude of 1.06×10^{-3} for 5000 cycles. (a) Viewed from the front surface; (b) viewed from the lateral surface.

3.3. Fatigue fractography observation

To further reveal the fatigue cracking process on different surfaces, fatigue fractographies of the bicrystals were observed by SEM. Fig. 4a shows the fractographies of the bicrystals cyclically deformed at axial plastic strain amplitude of 1.35×10^{-3}. Three regions (A, B, C) with different features can be seen. Wherein, region A is very smooth compared to regions B and C, and may be associated with full GB cracking. Meanwhile, the left side of region A corresponded to the front surface of the bicrystal. Region B became relatively rough but is still flatter than region C. It is apparent that fatigue crack propagation is from left to right in the Fig. 4a. Further observations (Fig. 4b) show that region D is very rough and corresponded to the zigzag path in Fig. 3b on the lateral surface. Apparently, region D should resulted from fatigue crack propagation through the lateral surface of the bicrystal. These observations provide powerful evidence for the tendency towards intergranular fatigue cracking on different surfaces, i.e. intergranular fatigue cracking on the front surface must be easier than that on the lateral surface in the present bicrystal.

3.4. Geometrical conditions for intergranular cracking

Based on the intergranular cracking in polycrystals, Christ [10] concluded that the possibility of intergranular cracking should be associated with the interaction angles (α, β) of PSB with GB and stress axis. The relations of PSB, GB and stress axis are shown in Fig. 5. He considered that the external axial stress σ leading to intergranular cracking in polycrystals is a function of α and β, i.e.

$$\sigma = K(\cos\alpha\cos(90° - \alpha)^{-1})(5 + 2\cos\beta - 3\cos^2\beta)^{-1/2} \quad (1)$$

Where K is a constant of materials and equal to

$$K = \left(\frac{2\pi\gamma G}{(1-\upsilon)\,\mathrm{d}}\right)^{1/2} \quad (2)$$

From Eq. (1), it can be known that the external axial stress σ will reach a minimum value as $\cos\alpha = \sqrt{2}/2$ and $\cos\beta = 1/3$. This means that when $\alpha = 45°$ and $\beta = 70.5°$, the minimum stress leading to intergranular cracking will be equal to

$$\sigma_{\min} = \sqrt{3\,\mathrm{K}}/2 \quad (3)$$

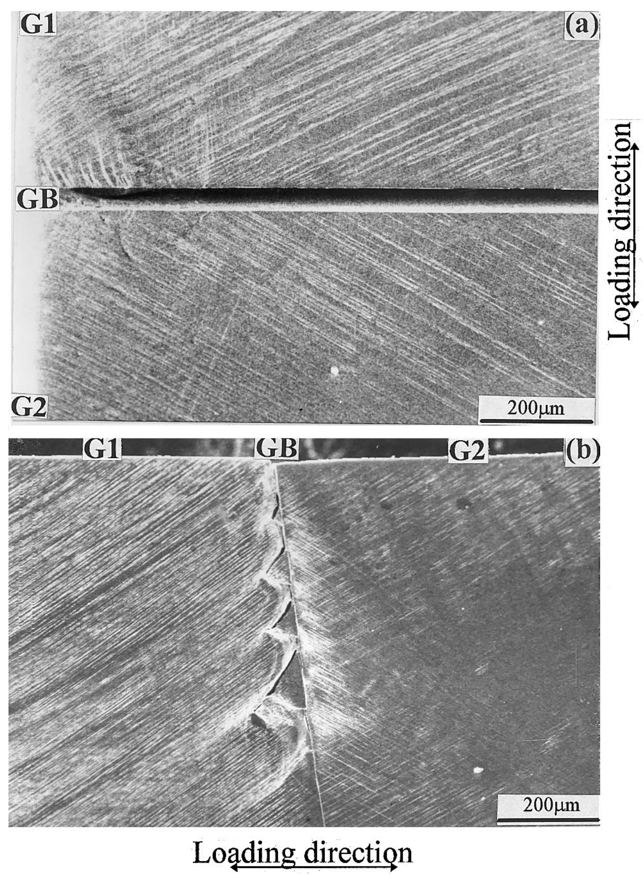

Fig. 3. Intergranular fatigue cracking in [$\bar{5}$913]⊥[$\bar{5}$79] copper bicrystal cyclically deformed at axial plastic strain amplitude of 1.35×10^{-3} for 10000 cycles. (a) Viewed from the front surface; (b) viewed from the lateral surface.

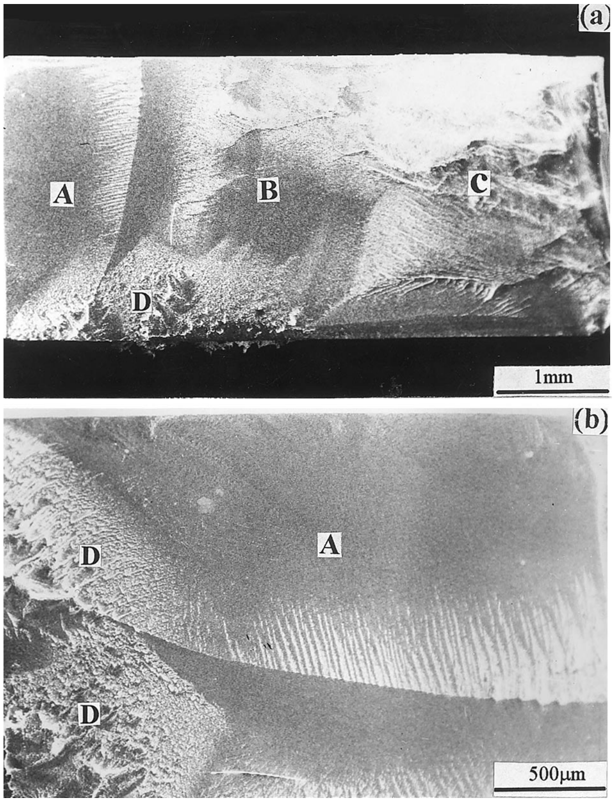

Fig. 4. Fatigue fractographies of [$\bar{5}$913]⊥[$\bar{5}$79] copper bicrystal. (a) Low magnification; (b) high magnification.

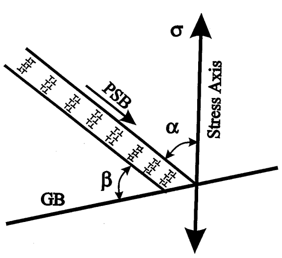

Fig. 5. Sketch of the geometrical relations among PSB, GB and stress axis.

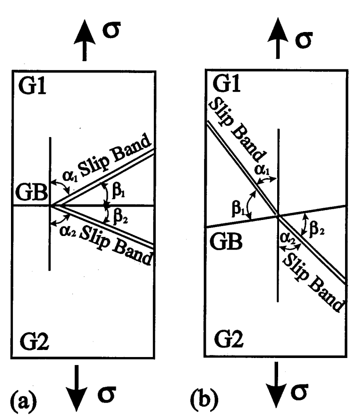

Fig. 6. The geometrical relations among slip bands, GB and stress axis in the copper bicrystal. (a) On the front surface; (b) on the lateral surface.

Therefore, Christ [10] suggested that intergranular cracking should be most preferential along the GB with the geometrical conditions of $\alpha = 45°$ and $\beta = 70.5°$. Based on the principle above, Hu and Wang [4] investigated the fatigue cracking feature of a [$\bar{3}$45]⊥[$\bar{1}$17] copper bicrystal with a GB perpendicular to the stress axis. They found that the number of fatigue cracks on one surface was always higher than that on another surface during cyclic deformation of the bicrystal. By comparing the number of fatigue cracks with the geometrical conditions among PSB, GB and stress axis on different surfaces of the [$\bar{3}$45]⊥[$\bar{1}$17] bicrystal, it was found that the geometrical conditions among PSB, GB and stress axis on the surface with higher number of cracks was very close to $\alpha = 45°$ and $\beta = 70.5°$. However, on the other surface of the [$\bar{3}$45]⊥[$\bar{1}$17] copper bicrystal, the geometrical conditions among PSB, GB and stress axis was obviously far from $\alpha = 45°$ and $\beta = 70.5°$. Consequently, they concluded that Christ's geometrical conditions for intergranular cracking was also suitable for the [$\bar{3}$45]⊥[$\bar{1}$17] copper bicrystal.

In the present [$\bar{5}$913]⊥[$\bar{5}$79] copper bicrystal, however, intergranular fatigue cracking displayed a more serious tendency than that in [$\bar{3}$45]⊥[$\bar{1}$17] copper bicrystal, as shown in Fig. 3. Therefore, intergranular fatigue cracking features of the bicrystal can also be investigated by using Christ's geometrical conditions. The geometrical relations among PSB, GB and stress axis on different surfaces in [$\bar{5}$913]⊥[$\bar{5}$79] copper bicrystal are shown in Fig. 6a, b, respectively. The values of α and β were measured and are listed in Table 1. It can be seen that on the front surface, the values of α and β are equal to 63 and 27° (within grain G1), and 61 and 29° (within grain G2), respectively. Those values are far from 45 and 70.5°. However, on the lateral surface, the values of α and β are equal to 37 and 64° (within grain G1), and 34 and 67° (within grain G2), respectively. Those values are very close to 45 and 70.5°. If considering Christ's geometrical conditions among PSB, GB and stress axis, it seems that intergranular fatigue cracking on the lateral surface should be more preferential than that on the front surface in [$\bar{5}$913]⊥[$\bar{5}$79] copper bicrystal. Unfortunately, in the present study, intergranular fatigue cracking always initiated along the GB at first on the front surface other than on the lateral surface, as shown in Fig. 3 and Fig. 4. Surface and fractography observations had supported powerful evidence for this. Apparently, the tendency towards intergranular fatigue cracking in [$\bar{5}$913]⊥[$\bar{5}$79] bicrystal provides evidence against Christ's geometrical conditions.

To further clarify the effect of geometrical conditions among PSB, GB and stress axis on intergranular fatigue cracking, the values of α and β in Table 1 were substituted into Eq. (1) to calculate the external axial stress σ leading to intergranular cracking. The calculated results

are also listed in Table 1. It can be seen that both stresses (1.18 and 1.12 K) within G1 and G2 grains leading to intergranular cracking on the front surface are higher than those (0.90 and 0.94 K) on the lateral surface. It is indicated that intergranular cracking on the lateral surface should be also easier than that on the front surface according to Christ's principle. However, intergranular fatigue cracking features in $[\bar{5}913]\perp[\bar{5}79]$ copper bicrystal was not consistent with Christ's geometrical conditions. This means that Christ's geometrical conditions of $\alpha = 45°$ and $\beta = 70.5°$ favorable to intergranular cracking are not suitable to $[\bar{5}913]\perp[\bar{5}79]$ copper bicrystal. The difference in intergranular cracking tendency between $[\bar{5}913]\perp[\bar{5}79]$ and $[\bar{3}45]\perp[\bar{1}17]$ copper bicrystals may be attributed to the following reasons.

It seems not suitable to verify Christ's geometrical conditions for intergranular cracking by using bicrystals. The interaction angles of α and β among PSB, GB and stress axis on different surfaces of a bicrystal have great differences, but the slip planes can penetrate the whole grains in a bicrystal during cyclic deformation. Obviously, the slip bands on the lateral surface are coplanar with those on the front surface. Hence, comparison of the difference in stress leading to intergranular cracking on different surfaces of a bicrystal has no significance.

The second case is that Christ's geometrical conditions might be further developed and the interaction mode of PSB with GB sometimes play a more important role in intergranular cracking during cyclic deformation. For the $[\bar{3}45]\perp[\bar{1}17]$ copper bicrystal, multiple slip occurred on the whole surfaces including the vicinity of GB. The interactions of secondary slip bands with GB and the primary slip bands were very complicated [4,5]. Obviously, the secondary slip bands may also interfere with intergranular cracking process in $[\bar{3}45]\perp[\bar{1}17]$ copper bicrystal. Therefore, the tendency towards intergranular cracking in $[\bar{3}45]\perp[\bar{1}17]$ copper bicrystal should not support convincing evidence for Christ's geometrical conditions. For the $[\bar{5}913]\perp[\bar{5}79]$ copper bicrystal, however, only the primary slip systems within grains G1 and G2 were activated on the whole surfaces during cyclic deformation. In this case, the geometrical conditions among PSB, GB and stress axis are very simple and secondary slip bands will have no effect on intergranular cracking. Meanwhile, on the lateral surface of $[\bar{5}913]\perp[\bar{5}79]$ copper bicrystal, it should be noted that the slip bands within grain G1 are nearly in line with those within grain G2 (Fig. 2 b). Whereas, on the front surface, the slip bands within G1 and G2 grains are at a great angle (Fig. 2 a). Therefore, the degree of plastic strain incompatibility on the front surface might be higher than that on the lateral surface during cyclic deformation. This may be the reason why intergranular fatigue cracking on the front surface was easier than that on the lateral surface. It is suggested that the plastic strain incompatibility caused by slip bands near a GB should be considered and Christ's geometrical conditions need to be further developed.

4. Conclusions

Based on the experimental results above, the following conclusions can be drawn.

(1) Only the primary slip system was activated on both grains G1$[\bar{5}913]$ and G2$[\bar{5}79]$ including the vicinity of the GB in the $[\bar{5}913]\perp[\bar{5}79]$ copper bicrystal during cyclic deformation.

(2) Surface and fractography observations in the $[\bar{5}913]\perp[\bar{5}79]$ copper bicrystal provided clear evidence of the tendency towards intergranular fatigue cracking on different surfaces. On the lateral surface, fatigue cracking along GB is more difficult than that on the front surface. By comparing the relations among PSB, GB and stress axis, it is suggested that the effect of plastic strain incompatibility caused by slip bands near a GB on intergranular fatigue cracking should be considered and Christ's geometrical conditions need to be further developed.

Acknowledgements

This work was financially supported by the National Natural Science Foundation of China (NSFC) under Grant Nos. 59701006 and 19392300-4. The authors are grateful for that support.

Table 1
Interaction angles (α and β) among PSB, GB and stress axis and the calculated stress leading to intergranular cracking in the $[\bar{5}913]\perp[\bar{5}79]$ copper bicrystal

	$[\bar{5}913]$ grain (G1)			$[\bar{5}79]$ grain (G2)		
	α_1 (°)	β_1 (°)	σ (K)	α_1 (°)	β_1 (°)	σ (K)
Front surface	63	27	1.18	61	29	1.12
Lateral surface	37	64	0.90	34	67°	0.94

References

[1] W.H. Kim, C. Laird, Acta Metall. 26 (1978) 789.
[2] L.C. Lim, Y.K. Tay, H.S. Fong, Acta Metall. Mater. 38 (1990) 595.
[3] W. Liu, M. Bayerlein, H. Mughrabi, A. Day, P.N. Quested, Acta Metall. Mater. 40 (1992) 1763.
[4] Y.M. Hu, Z.G. Wang, Scripta Mater. 34 (1996) 1019.
[5] Y.M. Hu, Z.G. Wang, Acta Mater. 45 (1997) 2655.
[6] P. Peralta, C. Laird, Acta Mater. 46 (1998) 2001.
[7] Z.F. Zhang, Z.G. Wang, S.X. Li, Fatigue Fract. Eng. Mater. Struct. 21 (1998) 1307.
[8] Z.F. Zhang, Z.G. Wang, Phil. Mag. 79A (1999) 741.
[9] H. Mughrabi, F. Ackermann, K. Herz, ASTM STP 811 (1983) 5.
[10] H.-J. Christ, Mater. Sci. Eng. A117 (1989) L25.